Published by :
https://www.ijert.org/
An International Peer-Reviewed Journal

International Journal of Engineering Research & Technology (IJERT)
ISSN: 2278-0181
Vol. 15 Issue 08 , August - 2026

Multivariate Performance Evaluation of CPRI based BBU Feed-In for Indoor Active DAS

Syed Muhammad Ali Moazzam Pasha
Mobile Services Provider, KSA

ABSTRACT

Cellular deployments in multilayered dense sharing environments can be challenging from power and infrastructure footprint requirements. One of the most pressing issues in Hybrid Indoor deployments is the realization of a sustainable and shareable Distributed Antenna System (DAS) with an optimized wattage, thereby limiting the carbon footprint and also enabling a commercially viable infrastructure viz a viz improved spectral efficiency and higher payload delivery per watt and acreage. A direct CPRI interface with the processing units in a typical topology circumvents the need for Radio Transceivers before the head end, which helps in alleviating high power consumption and space. This however requires benchmarking performance, most notably the effects of Cascaded Error Vector Magnitude (EVM) and Uplink (UL) Noise since these are some of the most fundamental Physical layer determinants for payload delivery and spectral efficiency. This paper intends to evaluate the effects of these two based on some readily available performance KPIs and employ statistical techniques to view the impact for direct CPRI interface at a higher level of abstraction.

I. INTRODUCTION

The rapid growth of indoor mobile traffic and high-capacity venues such as airports, hospitals, stadiums, and commercial complexes have significantly increased the demand for high-performance Indoor Building Systems (IBS). The distributed antenna system (DAS) has become the preferred solution for providing seamless indoor coverage and higher capacity; however, the large number of active network elements required in conventional active and hybrid DAS deployments has also resulted in increased energy consumption, operational expenditure (OPEX) and infrastructure complexity. As mobile operators continue to pursue sustainable networks, reducing the energy footprint of indoor radio access infrastructure has become an important research and operational objective. But most importantly, with increased complexity, the number of cascaded nodes and active components has led to increased distortions and noise defined by Error Vector Magnitude (EVM) and Noise Rise Values (NRV). Considerable research has focused on improving the energy efficiency of base stations, but this paper investigates the impact of Direct BBU Feed-In as a means of improving system spectral efficiency and radio link quality due to improved EVM and UL noise. While measuring the EVM is costly and requires specialized instruments, proxy performance indicators can help in benchmarking and this paper provides an Machine Learning based approach to ascertain whether direct BBU feed-in solutions circumvents these issues in link quality.

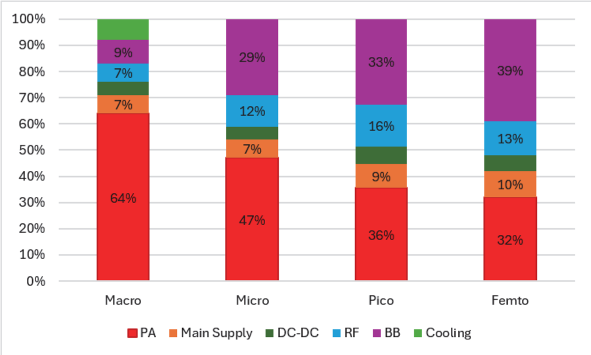

Fig. 1. Power Consumption distribution in different types of Base Stations.

A. Cellular Energy Consumption

As illustrated in Fig. 1 , the Power Amplifier (PA) constitutes the largest single contributor to base station energy consumption, accounting for approximately 47% of the power consumption in micro base stations and 36% in pico base stations. Although active and hybrid Indoor Building System (IBS) architectures are not identical to standalone micro or pico base stations, their radio front-end architectures share many common functional blocks, including RF transceiver chains, power amplification and baseband processing. Consequently, the power consumption breakdown of micro and pico base stations provides a useful approximation of the relative contribution of the PA stage in active indoor radio equipment [1].

B. Hybrid DAS Effective Power Requirement

Unlike outdoor cellular deployments, where high RF transmit power is required to overcome large propagation losses and provide wide-area coverage, hybrid Active DAS primarily functions as a signal distribution network. Radio Transmit power required at the DAS interface remains significantly lower than that of a conventional outdoor base station because the radio signal is converted into low power optical signal with input power requirement usually around 0 dBm. Consequently, the use of a high-power amplification stage represents a substantial architectural overhead for many IBS deployments.

C. Direct BBU Feed-In

This observation provides the motivation for the proposed Direct BBU Feed-In architecture, in which the distributed antenna network is driven directly from the centralized Baseband Unit (BBU), thus eliminating the intermediate PA stage traditionally employed within the Active DAS architecture. Figures 2 and 3 depict the two architectures showing that the complete Power Amplifiers- Radio stage is removed in the direct BBU feed-in architecture. The CPRI specification [2] provides a framework

International Journal of Engineering Research & Technology (IJERT)
ISSN: 2278-0181
Vol. 15 Issue 08 , August - 2026

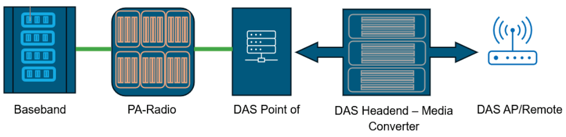

Fig. 2. Conventional RF Feed-In DAS Architecture.

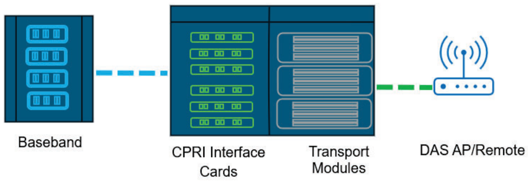

Fig. 3. CPRI Based BBU Feed-In DAS Architecture.

for this implementation but details of actual implementation are subject to original equipment manufacturers (OEMs) interfaces and are beyond the scope of this paper. Nevertheless the proposed architecture has the potential to substantially reduce the overall energy consumption of IBS deployments. But beyond energy savings, the removal of an active amplification stage reduces the introduction of nonlinear distortion [5], offering the potential for improved uplink Noise and Error Vector Magnitude (EVM). These advantages make Direct BBU Feed-In an attractive architecture for next-generation energy-efficient indoor wireless networks, particularly as operators seek to reduce the operational expenditure while also evaluating the complete RF chain rather than an individual PA in isolation [4].

II. RADIO LINK IMPAIRMENTS : EFFECTS OF CASCADED ACTIVE NODES

A. Cascaded EVM

Error Vector Magnitude (EVM) is a fundamental performance metric that quantifies the modulation accuracy of a wireless transmitter or receiver by measuring the deviation between the received modulation symbols and their ideal constellation points. In practical radio systems, EVM represents the cumulative effect of RF impairments introduced throughout the signal chain, including power amplifier (PA) non-linearity, phase noise, IQ imbalance, local oscillator instability, quantization noise, thermal noise, and frequency-dependent distortion. Since modern cellular systems employ cascaded RF architectures comprising multiple active and passive components, the overall EVM reflects the aggregate distortion introduced by each stage.

Recent work [4] demonstrated that the EVM generated by a non-linear power amplifier cannot be considered independently from the surrounding RF network. Their system-level analysis showed that when a non-linear PA is cascaded with a generic linear network, such as impedance matching circuits, filters, couplers, or distribution networks, the resulting EVM depends on the combined response of the entire RF chain rather than the PA alone. Their experimental wideband load-pull measurements further demonstrated that impedance mismatch can significantly increase the measured EVM over wide modulation bandwidths, highlighting the importance of evaluating the complete transmission chain rather than individual components in isolation.

For cellular systems such as LTE and NR, degradation in EVM has a direct impact on receiver Signal-to-Interference-plus-Noise Ratio (SINR). Although EVM is fundamentally a modulation quality metric rather than a power ratio, the distortion represented by EVM behaves as an additional interference component that reduces the spectral effciency of the system. Under the assumption that distortion sources are uncorrelated with the desired signal, the relationship can be approximated by

$$\mathrm{SINR_{eff}} \approx \frac{1}{\mathrm{EVM}^2}, \tag{1}$$

where EVM is expressed as a linear quantity rather than a percentage. Consequently, increasing EVM reduces the effective SINR available for demodulation, even when the received signal strength remains unchanged.

The reduction in effective SINR directly impacts the achievable spectral efficiency of LTE and NR systems. According to Shannon's capacity relationship,

$$\eta = \log_2(1 + \mathrm{SINR}), \tag{2}$$

where η represents the achievable spectral efficiency in bits/s/Hz. A decrease in SINR due to higher EVM therefore reduces the maximum achievable throughput for User Equipment (UE). In practical LTE systems, this manifests as the scheduler selecting a lower Modulation and Coding Scheme (MCS), transitioning, for example, from 256-QAM to 64-QAM or from 64-QAM to 16-QAM in order to satisfy Block Error Rate (BLER) requirements. The reduction in modulation order and coding rate subsequently decreases user throughput and cell capacity.

This relationship is particularly significant for Active Distributed Antenna Systems (DAS), where the transmitted signal is cascaded through multiple active RF stages before reaching the distributed antennas. Each additional amplifier, frequency conversion stage, or active remote unit contributes incremental distortion and noise, producing what may be termed cascaded EVM. Although no universal analytical expression exists for cascaded EVM, an empirical alternative could be the RSS of EVM for all stages.

$$\mathrm{EVM_{total}} = \sqrt{\mathrm{EVM}_1^2 + \mathrm{EVM}_2^2 + \mathrm{EVM}_3^2 + \cdots}. \tag{3}$$

The cumulative impairment increases the effective distortion observed at the receiver, reducing SINR and ultimately limiting the achievable throughput.

B. Cascaded Uplink Noise

The Uplink (UL) noise floor of a wireless communication system represents the minimum level of unwanted electrical noise present at the receiver input that limits the detection of weak signals. In practical cellular radio systems, the receiver noise floor is not determined by a single component but rather by the cumulative contribution of all active and passive elements within the receive chain. Low Noise Amplifiers (LNAs), duplexers, filters, mixers, variable gain amplifiers (VGAs), cables, couplers, repeaters and distributed antenna equipment each introduce additional thermal noise and attenuation, collectively increasing the overall receiver noise figure (NF). This cumulative degradation is commonly referred to as the cascaded noise figure or cascaded noise floor, and is fundamentally described by the Friis cascade equation [6].

For a receiver comprising cascaded stages, the overall noise

International Journal of Engineering Research & Technology (IJERT)
ISSN: 2278-0181
Vol. 15 Issue 08 , August - 2026

factor is expressed as

$$F_{\text{total}} = F_1 + \frac{F_2 - 1}{G_1} + \frac{F_3 - 1}{G_1 G_2} + \cdots + \frac{F_N - 1}{\prod_{i=1}^{N-1} G_i}, \quad (4)$$

where F_i and G_i denote the noise factor and gain of stage i, respectively. The Friis equation demonstrates that the first few stages of the receiver chain dominate the overall system noise figure, emphasizing the importance of low-noise front-end design. Conversely, passive losses occurring before the first amplification stage directly increase the receiver noise figure because attenuation degrades both signal power and signal-to-noise ratio before amplification.

In LTE and 5G cellular systems, an increase in cascaded noise floor directly reduces the effective receiver Signal-to-Interference-plus-Noise Ratio (SINR). As the cascaded noise floor increases, weaker user signals become increasingly difficult to distinguish from the background noise, particularly for users located near the cell edge or within high-loss indoor environments. The reduction in effective SINR forces the scheduler to select more robust but lower-order Modulation and Coding Schemes (MCS), reducing the achievable spectral efficiency and ultimately decreasing user throughput.

This relationship is well established in LTE receiver design. For example, [7] demonstrates cascaded noise figure analysis for an LTE receiver front-end consisting of duplexers, LNAs, mixers, filters and variable gain amplifiers. The analysis shows how each stage contributes to the cumulative receiver noise figure, which directly determines receiver sensitivity and carrier-to-noise ratio. The same methodology is subsequently used to calculate the minimum detectable LTE signal level, illustrating the direct relationship between cascaded noise figure, receiver sensitivity and communication performance.

The impact of cascaded noise is particularly relevant in Indoor Building Systems (IBS) employing Active or Hybrid Distributed Antenna Systems (DAS). According to Friis' cascaded noise equation, the overall receiver noise figure depends not only on the noise figure of each stage but also on the gain of the preceding stage. Passive insertion losses introduced by splitters, couplers, duplexers, and attenuators directly increase the effective system noise figure because they attenuate the received signal before subsequent amplification. By eliminating the high-power RF transmission stage and feeding the Active DAS directly from the BBU, RF attenuation and associated cascade losses are reduced and thus improving receiver sensitivity and uplink SINR. Conversely, the cumulative effect of higher receiver noise floor reduces the uplink SINR and results in increased uplink Block Error Rate (BLER), lower Channel Quality Indicator (CQI), reduced spectral efficiency and lower user throughput. Removing one of the primary sources of RF non-linearity, the PA stage, reduces the accumulated EVM while simultaneously lowering thermal noise generation.

III. BENCHMARKING FRAMEWORK

To quantify the impact of the proposed Direct BBU Feed-In architecture on indoor cellular network performance, a rudimentary performance evaluation framework was developed using operational Key Performance Indicators (KPIs) collected from commercial Indoor Building System (IBS) deployments. The study compares indoor sites employing the proposed Direct BBU Feed-In architecture against conventional hybrid Active DAS deployments utilizing the legacy BBU–RF feed-in architecture. Since the proposed architecture fundamentally modifies the RF signal chain by eliminating the intermediate power amplifier stage, the evaluation focuses on network-level performance indicators that directly reflect improvements in signal quality and user experience.

TABLE 1. Significance of Performance Indicators and Expected Impact of Direct BBU Feed-In

KPI	Layer	Expected Impact	Primary RF Mechanism
DL/UL SINR	Physical	↑	Reduced cascaded EVM and receiver noise
Average CQI	Physical	↑	Improved signal quality
DL/UL BLER	Link	↓	Improved demodulation and decoding
DL/UL Packet Loss	Link	↓	Fewer HARQ retransmissions and decoding failures
DL Spectral Efficiency	MAC/PHY	↑	Higher MCS selection
DL/UL Throughput	User	↑	Higher spectral efficiency and lower retransmissions
Average UE Headroom	Uplink	↑	Improved uplink sensitivity and lower required UE transmit power

A. Layer 1 Metrics Overview

Physical layer or Layer 1 metrics such as Downlink Spectral Efficiency and Uplink (UL) Signal-to-Interference-plus-Noise Ratio (SINR), Average Channel Quality Indicator (CQI), UE Power Headroom, in addition to other performance indicators such as actual Cell Average Throughput and Average CQI, are used to quantify improvements in radio signal quality resulting from reductions in cascaded Error Vector Magnitude (EVM) and noise floor. Link-layer performance is also evaluated using Downlink and Uplink Block Error Rate (BLER). These metrics characterize the reliability of the radio link and provide an indication of the quality of Radio Link

Collectively, these KPIs enable the proposed architecture to be evaluated from multiple complementary perspectives.

IV. STATISTICAL METHODOLOGY AND DATASET

Statistical analysis focused on first establishing the ground truth about supposed improvements in the performance of Direct BBU feed-in systems in comparison to the legacy RF Feed-in systems. Then the approach is to classify the two solutions in relation to the performance and visualize how distinct the two systems are. For this study a total of 52 cells were selected with 28 cells with a working direct BBU feed in solution to the DAS. All cells had comparable traffic and connected users, two factors which can influence the KPIs. The data was based on an hourly resolution with 9563 independent observation for the 52 cells with each data point consisting of 18 performance measurements such as UL/DL Cell throughput, DL Spectral Efficiency, UL SINR, UL/DL BLER etc.

A. Linear Mixed-Effect Model

To establish a statistical baseline prior to the multivariate analysis, a Linear Mixed-Effects Model (LMM) was employed to quantify the influence of the deployment architecture on the selected downlink and uplink KPIs. The model accounts for

International Journal of Engineering Research & Technology (IJERT)
ISSN: 2278-0181
Vol. 15 Issue 08 , August - 2026

TABLE 2. Mixed-Effects Model Results

KPI	Architecture		Users	
	Effect	p	Effect	p
DL Spectral Efficiency	+0.6113	3.88×10^{-4}	+0.0496	$< 10^{-16}$
DL Throughput	+5.4606	2.06×10^{-6}	+0.4165	$< 10^{-16}$
DL BLER	+0.0335	0.0380	-0.00110	0.300
Average CQI	-0.1261	0.704	+0.00776	5.85×10^{-4}
UL SINR (PUSCH)	+4.863	6.79×10^{-15}	+0.1423	$< 10^{-15}$
UL Throughput	+2.0355	0.0246	+0.0208	0.726
UL BLER	+0.1228	0.0192	+0.00020	0.955
Average UE Headroom	-2.1286	0.0949	+0.0237	0.0206

the repeated hourly observations collected from each cell by treating cell identity as a random effect, while deployment architecture (0 = legacy BBU-RF Feed-In, 1 = Direct BBU Feed-In) and connected users were modeled as fixed effects. Consequently, the estimated architecture coefficient represents the average performance difference between the two deployment architectures after accounting for variations in traffic load and cell-specific characteristics.

$$Y_{ij} = \beta_0 + \beta_1 A_{ij} + \beta_2 U_{ij} + u_j + \epsilon_{ij}, \quad (5)$$

where A_{ij} denotes the deployment architecture, U_{ij} represents the Average Connected Users, u_j is the random intercept associated with cell j, and ϵ_{ij} is the residual error.

B. Univariate Performance Results

The preliminary mixed-effects analysis indicates that Direct BBU Feed-In is primarily associated with improvements in Radio performance metrics. After adjusting for differences in traffic load, statistically significant gains are observed in DL Spectral Efficiency (+0.61 bps/Hz), DL Throughput (+5.46 Mbps), UL SINR (+4.86 dB), and UL Throughput (+2.04 Mbps). These improvements persist after accounting for connected Users, suggesting that the observed performance gains cannot be attributed solely to differences in network loading.

Conversely, Average CQI and Average UE Headroom do not exhibit statistically significant dependence on deployment architecture, while both DL and UL BLER require further investigation since the estimated direction of the architecture coefficient does not fully align with the improvements observed in throughput and SINR. These results suggest that the principal impact of Direct BBU Feed-In is reflected in downlink and uplink payload delivery capability while secondary metrics such as BLER, CQI and UE headroom not exhibiting any statistically significant dependency. These results are compiled in Table 2

V. MULTIVARIATE PERFORMANCE ANALYSIS

While the mixed-effects model provides statistical evidence of the independent influence of the deployment architecture on individual KPIs, it evaluates each performance indicator separately. Cellular network performance is inherently multidimensional, with capacity, radio quality, reliability, and traffic load interacting simultaneously. So the next stage of the analysis extends beyond individual KPI comparisons and employs multivariate techniques to investigate the combined effect on these indicators. This enables the identification of latent cavrying dimensions and performance patterns associated with Direct BBU Feed-In and conventional BBU-RF Feed-In deployments. This provided a more comprehensive understanding

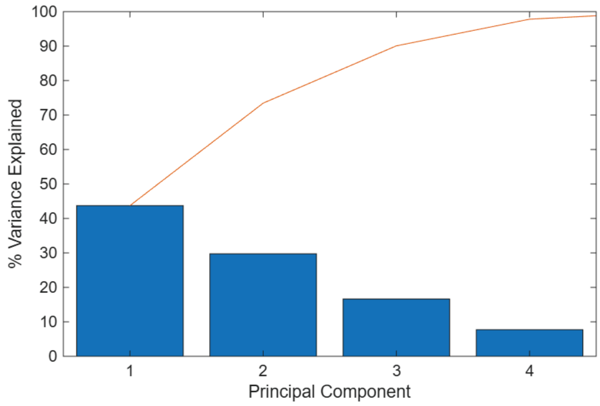

Fig. 4. First 3 Principal Components explain 90 Percent Variance

and classification of the architectural differences.

A. Multivariate Performance Analysis

To complement the mixed-effects analysis, a multivariate workflow was used to investigate whether the selected KPIs collectively formed distinct operating clusters associated with the two indoor deployment architectures. Prior to dimensionality reduction, multivariate outliers were identified and removed using robust statistical criteria. A total of 324 observations (3.23%) were classified as outliers and excluded from further analysis. The relatively small proportion of discarded samples indicates that the dataset was largely representative of normal network operation while eliminating observations that could disproportionately influence the latent feature extraction.

B. Principal Component Analysis

Following outlier removal, Principal Component Analysis (PCA) was applied to the standardized KPI dataset comprising downlink spectral efficiency, downlink throughput, uplink throughput, uplink SINR, average CQI, and UE headroom. PCA was employed to transform the correlated KPI space into a reduced set of orthogonal latent variables while preserving the majority of the information contained in the original measurements. The first three principal components accounted for the overwhelming proportion of the total variance and were therefore selected for subsequent visualization and clustering. The resulting three-dimensional latent space revealed two partially overlapping but visibly shifted groups, suggesting that the two deployment architectures exhibit different multivariate operating characteristics despite sharing common traffic conditions and propagation environments.

C. Gaussian Mixture Model

In Fig. 5, the multivariate KPI observations exhibited overlapping and approximately bimodal behavior. Thus a Gaussian Mixture Model (GMM) was selected to identify the underlying performance regimes. Unlike hard-partitioning methods such as K-means, GMM allows observations to have probabilistic classification in multiple clusters and can therefore accommodate the observed overlap between the two regimes. The bimodal structure further suggested that a two-component GMM was an appropriate model for characterizing the underlying performance populations.

To objectively identify these operating regimes without using any prior knowledge of the deployment architecture, an unsupervised Gaussian Mixture Model (GMM) was trained

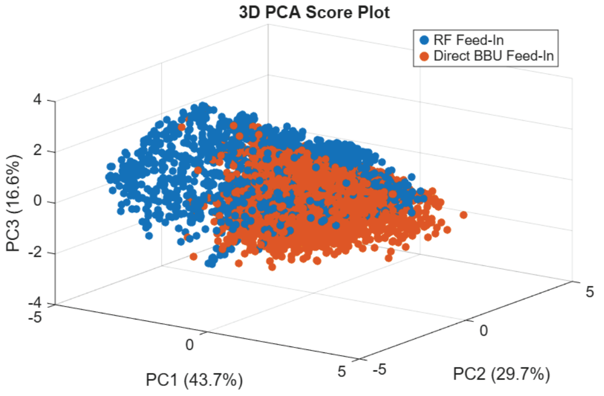

Fig. 5. Original Clusters for RF and BBU Feed-In

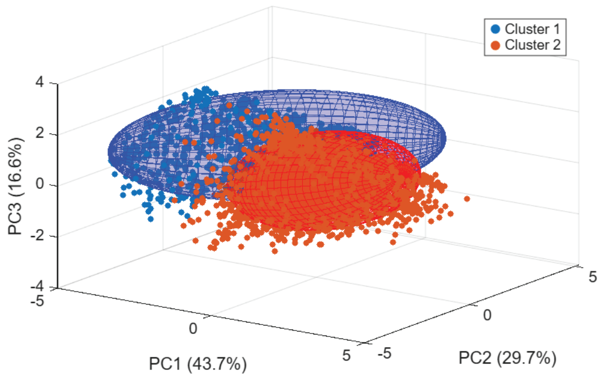

Fig. 7. Clustering based on GMM

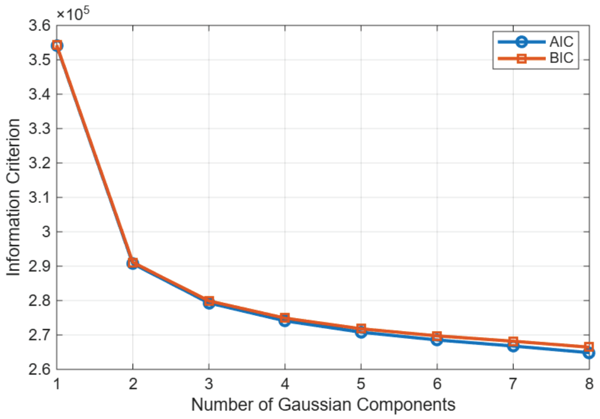

Fig. 6. AIC-BIC criterion for clusters count

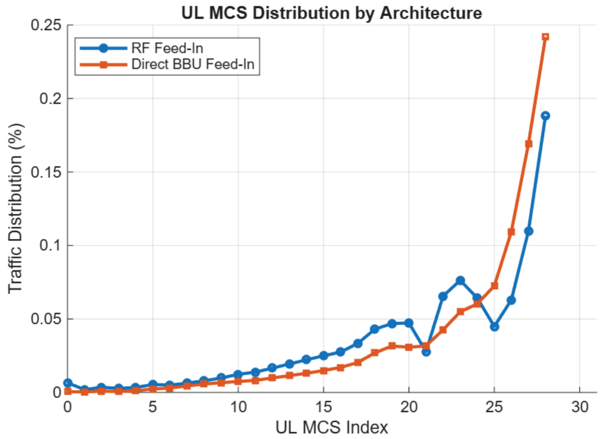

Fig. 8. Higher MCS Values for BBU Feed-In

using the first three principal components. The optimal number of Gaussian components was determined using the Akaike Information Criterion (AIC) and Bayesian Information Criterion (BIC), both of which exhibited an elbow at two components. Fig. 6, indicating that a two-cluster solution provided the best balance between model complexity and goodness-of-fit. This validates the original two architecture explainability derived from the mixed effects linear model.

The resulting GMM partitioned the observations into two predominant multivariate operating regimes as shown in Fig 7. Although the clusters exhibited partial overlap, reflecting the common operating environment of indoor LTE networks, a clear association with the deployment architecture was observed. Approximately 84% of the legacy RF Feed-In observations were assigned to the corresponding operating regime, whereas 63% of the Direct BBU Feed-In observations were assigned to the second regime. The higher classification rate for RF Feed-In suggests that its performance characteristics are comparatively homogeneous, while the lower classification rate for Direct BBU Feed-In indicates greater variability in operating conditions. This behaviour is expected, as Direct BBU Feed-In sites encompass a broader range of traffic loads and deployment scenarios, resulting in a wider spread in the latent KPI space.

Overall, the multivariate analysis provides independent evidence that the two deployment architectures occupy systematically different regions of the KPI feature space. Unlike the mixed-effects models, which quantify the impact of deployment architecture on individual KPIs after controlling for traffic load, the PCA-GMM framework demonstrates that these KPI improvements collectively manifest as distinct multivariate operating regimes. Consequently, the clustering results reinforce the statistical findings of the mixed-effects models and indicate that the performance gains associated with Direct BBU Feed-In are not confined to isolated KPIs but represent a broader shift in overall network operating behaviour.

VI. MCS DISTRIBUTION ANALYSIS

The MCS distribution analysis provides a more granular view of the link-adaptation behavior of the two architectures. Across the 32 downlink MCS bins and 29 uplink MCS bins, the DL distributions show only subtle differences between RF Feed-In and Direct BBU Feed-In, with no clear observable shift in the distribution of pegged values. In contrast, the UL distribution exhibits a more distinct difference, Fig 8, with Direct BBU Feed-In showing a higher proportion of observations in the higher MCS bins. This shift is consistent with the higher UL SINR observed in the mixed-effects analysis and suggests that the improved uplink radio conditions associated with Direct BBU Feed-In may enable the scheduler to sustain more efficient modulation and coding levels.

VII. INFERENCE

A. RF Mechanism

The observed performance differences can be interpreted in terms of the RF architectures. Conventional RF Feed-In requires high-power RF transmission followed by attenuation and distribution through multiple RF components, introducing additional insertion losses. Direct BBU Feed-In reduces the dependence on this high-power RF chain and associated attenuation, providing a plausible explanation for the observed improvement in UL SINR and DL spectral efficiency, as validated by mixed effects model. Since cascaded EVM and UL noise were not directly measured in this study, these mechanisms should be regarded as engineering interpretations rather than directly measured effects.

B. Link Adaptation

The improvement in radio conditions associated with Direct BBU Feed-In is expected to influence LTE link adaptation through the selection of MCS levels. The observed increase in UL SINR and DL spectral efficiency suggests more favorable radio conditions for transmission. Analysis of the complete MCS distribution, rather than only the dominant MCS 29 bin, therefore provides a means of determining whether these improvements translate into greater utilization of higher MCS levels. The observed effect was more pronounced in UL where BBU Feed-In showed better performance than legacy RF Feed-In solution.

C. Network Performance

The mixed-effects results demonstrate that Direct BBU Feed-In is associated with improvements across several network-level KPIs after accounting for traffic load and cell-specific variability. In particular, Direct BBU Feed-In increased DL spectral efficiency by 0.611 bps/Hz, DL throughput by 5.46 Mbps, UL SINR by 4.86 dB, and UL throughput by 2.04 Mbps. The PCA-GMM analysis further showed two partially overlapping performance regimes, with 84% of RF Feed-In and 63% of Direct BBU Feed-In observations associated with their respective dominant regimes, providing complementary evidence of architecture-dependent performance characteristics.

D. Engineering Implications

The results indicate that Direct BBU Feed-In can provide both network-performance and architectural benefits by reducing reliance on high-power RF amplification and associated RF distribution components. The measured improvements in SINR, spectral efficiency, and throughput suggest that simplifying the RF chain does not compromise network performance and may provide measurable gains. In addition, removing unnecessary active RF stages has the potential to reduce equipment power consumption, thermal load, and space requirements. Direct power, EVM, and cascaded-noise measurements are nevertheless required to quantify these benefits independently.

VIII. LIMITATIONS AND FUTURE WORK

While the effects of variability due to traffic load and concurrent users have been factored into the mixed-effects model, Indoor DAS deployments can have different response to factors like network density, traffic profiles, clutter, proximity to outdoor Macro sites, ingress of outdoor Macro RF power etc. This can directly have an impact on performance which can diminish the effect of gains from architecture types. Ideally, benchmarking should be done on the same site in tandem but this can be challenging from deployment and prohibitive from commercial point of view. While results in a lab environment can be isolated from the external factors, system response to traffic and load gradient is possible only with live traffic.

IX. CONCLUSION

Multivariate analysis presented in this study provides a framework for evaluating Direct BBU Feed-In against legacy BBU-RF Feed-In architectures using operational KPIs. The mixed-effects results indicate statistically significant improvements in DL spectral efficiency, DL throughput, UL SINR, and UL throughput after accounting for traffic load and cell-specific variability. Analysis based on GMM further indicates that the two architectures occupy distinctly different, although partially overlapping, multivariate performance regions. MCS distribution analysis provides a further mechanism for investigating the radio-quality improvements in relation to LTE link adaptation. Direct measurements of power consumption, EVM, and cascaded noise remain necessary to independently quantify the underlying RF and energy mechanisms.

X. ACKNOWLEDGEMENT

Direct CPRI feed-In solutions are deployed by different DAS manufacturers and exact implementation varies for every vendor's commercial product. However, benchmarking framework has been developed independently based on performance metrics developed by cellular services provider for a Tier-1 ICT OEM supplier. The author has used AI-assisted tools for language editing and document structuring.

REFERENCES

[1] A. Gati et al., "Key technologies to accelerate the ICT Green evolution—An operator's point of view," arXiv:1903.09627, 2019, doi: 10.48550/arXiv.1903.09627.

[2] CPRI Cooperation, *CPRI Specification V6.0: Common Public Radio Interface (CPRI); Interface Specification*, Aug. 30, 2013. [Online]. Available: `http://www.cpri.info`

[3] Y. Josse, B. Fracasso, G. Castignani, and N. Montavont, "Energy-efficient deployment of Distributed Antenna Systems with Radio-over-Fiber link," *Reference details to be completed from the verified source*.

[4] G. P. Gibiino, A. M. Angelotti, A. Santarelli, and P. A. Traverso, "Error vector magnitude measurement for power amplifiers under wideband load impedance mismatch: System-level analysis and VNA-based implementation," *Measurement*, vol. 187, Art. no. 110254, 2022, doi: 10.1016/j.measurement.2021.110254.

[5] E. Uthirajoo, H. Ramiah, J. Kanesan, and A. W. Reza, "Wideband LTE Power Amplifier with Integrated Novel Analog Pre-Distorter Linearizer for Mobile Wireless Communications," *PLOS ONE*, vol. 9, no. 7, Art. no. e101862, 2014, doi: 10.1371/journal.pone.0101862.

[6] H. T. Friis, "Noise Figures of Radio Receivers," *Proceedings of the IRE*, vol. 32, no. 7, pp. 419–422, July 1944, doi: 10.1109/JRPROC.1944.232049.

[7] T. J. Rouphael, *Wireless Receiver Architectures and Design: Antennas, RF, Synthesizers, Mixed Signal, and Digital Signal Processing*. Oxford, U.K.: Newnes/Elsevier, 2014.